RSC Advances

PAPER

View Article Online
View Journal | View Issue

Cite this: *RSC Adv.*, 2021, **11**, 3183

Two lathyrane diterpenoid stereoisomers containing an unusual *trans-gem*-dimethylcyclopropane from the seeds of *Euphorbia lathyris*†

Linwei Li,‡[a] Jianan Huang,‡[a] Hui Lyu,[ab] Fuqin Guan,[a] Pirui Li,[a] Mei Tian,[a] Shu Xu,[a] Xingzeng Zhao,[a] Fei Liu,*[a] Christian Paetz,[b] Xu Feng[a] and Yu Chen *[a]

Received 22nd December 2020
Accepted 7th January 2021

DOI: 10.1039/d0ra10724g

rsc.li/rsc-advances

Two novel lathyrane-type diterpenoids, the *Euphorbia* factors L_{2a} (**1**) and L_{2b} (**2**), and their stereoisomer *Euphorbia* factor L_2 (**3**) were obtained from seeds of *Euphorbia lathyris*. Both *Euphorbia* factors L_{2a} and L_{2b} possess an unprecedented *trans-gem*-dimethylcyclopropane as structural feature. Also, the *Euphorbia* factor L_{2a} is the first example of a lathyrane diterpenoid with an endocyclic 12(*Z*)-double bond. The structures of the molecules and their absolute configurations were elucidated by comprehensive spectroscopic analyses, Cu-Kα radiation X-ray diffraction, and comparison with calculated electronic circular dichroism (ECD) data. The *Euphorbia* factor L_{2b} exhibited an inhibitory effect against U937 cell line with an IC_{50} value of 0.87 μM.

Introduction

Lathyrane diterpenoids, a group of macrocyclic diterpenoids based on a 5/11/3-tricyclic skeleton, have been found exclusively in the family Euphorbiaceae.[1] These diterpenoids contain a *cis*-fused *gem*-dimethylcyclopropane unit and are generally substituted with a variety of acyl groups.[2] Several studies have been conducted to investigate lathyrane diterpenoids for their anticancer,[3,4] multidrug resistance modulation (MDR),[5–7] and anti-inflammatory activities.[8,9] The existing structure–activity relationship (SAR) analyses showed that the configuration of the molecule's structure as well as the nature of the acyl side chains influence the bioactivities of lathyrane diterpenoids.[4,6,10] However, whether the configuration of the *gem*-dimethylcyclopropane influences the bioactivity of lathyrane diterpenoids has never been studied.

Euphorbia lathyris is native to the Mediterranean and has been introduced to many other parts of the world. A characteristic of the plant's constituents is the abundance of lathyrane-type diterpenoids. Up to now, 46 lathyrane-type diterpenoids, most of them containing an endocyclic 12(*E*)-double bond, have been identified.[7,8,11–14] As part of our ongoing search for bioactive natural products,[15–18] two novel lathyrane diterpenoids, the *Euphorbia* factor L_{2a} (**1**) and L_{2b} (**2**) along with the *Euphorbia* factor L_2 (**3**)[19] were isolated from the seeds of *E. lathyris*. The compounds **1–3** share the presence of similar planar structures, but the configuration of the *gem*-dimethylcyclopropanes and the endocyclic 12-double bonds differ. Herein, we describe the isolation, structural elucidation, and the cytotoxicity evaluation of the isolated compounds. The results indicate that the cytotoxicity of lathyrane-type diterpenoids is dependent on the configuration of the *gem*-dimethylcyclopropane and the endocyclic double bond.

Results and discussion

Seeds of *E. lathyris* (12 kg) were extracted with 95% aqueous ethanol. The extract was rotary-evaporated, reconstituted with H_2O and successively partitioned with petroleum ether, dichloromethane, and ethyl acetate. The petroleum ether-soluble fraction was re-extracted with acetonitrile. Then the acetonitrile fraction was subjected to separation by column chromatography on silica gel and (recycling) semipreparative HPLC to obtain compound **1** (45 mg), compound **2** (20 mg), and compound **3** (120 mg) (Fig. 1).

Structural elucidation of *Euphorbia* factors L_{2a} (1)

Compound **1**, obtained as colorless crystals, showed a specific optical rotation value of $[\alpha]_D$ +20.9 [*c* 0.50, methanol/CH_2Cl_2

[a]*Jiangsu Key Laboratory for the Research and Utilization of Plant Resources, The Jiangsu Provincial Platform for Conservation and Utilization of Agricultural Germplasm, Institute of Botany, Jiangsu Province and Chinese Academy of Sciences, Nanjing, China. E-mail: yuchen1007@hotmail.com; liufeiseu@163.com*

[b]*Max-Planck Institute for Chemical Ecology, Jena, Germany*

† Electronic supplementary information (ESI) available: HR-HPLC-ESI-MS, ^1H and ^{13}C NMR, ^{13}C-DEPT, ^1H–^{13}C HSQC, ^1H–^{13}C HMBC, ^1H–^1H COSY, ^1H–^1H NOESY data of compounds **1–3**, the DFT-optimized 3D structures of relative stable conformers of compound **2** and their Boltzmann weighting factors. CCDC 2010124 for the crystal structure of **1**. The CCDC contains the supplementary crystallographic data for this paper. For ESI and crystallographic data in CIF or other electronic format see DOI: 10.1039/d0ra10724g

‡ These two authors contributed equally to this work.

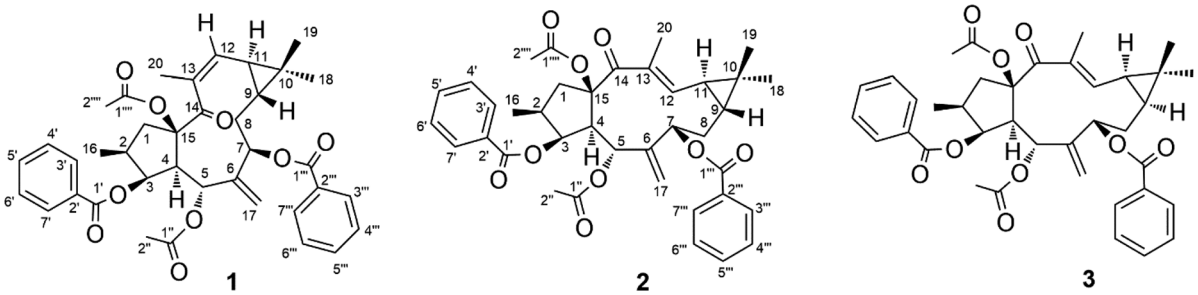

Fig. 1 Chemical structures of compounds **1–3**.

(95 : 5, v/v)]. The molecular formula of $C_{38}H_{42}O_9$ was determined by the pseudo-molecular ion peak at *m*/*z* 665.2720 [M + Na]$^+$ (calculated for $C_{38}H_{42}O_9Na$, 665.2721) in positive HR-ESI-MS. The ^{1}H NMR, ^{13}C NMR, and DEPT spectra of **1** (Table 1) exhibited signals for a ketone group, two acetyl groups, two benzoyl groups, two double bonds (one exocyclic and one trisubstituted), four methyls, two methylenes, seven methines (three oxygenated), and two quaternary carbons (one oxygenated). The interpretation of the above-mentioned spectra data suggested that compound **1** is an isomer of *Euphorbia* factor L_2

Table 1 ^{1}H and ^{13}C NMR spectral data of compounds **1–3** in $CDCl_3$

	1		**2**		**3**	
	$\delta_H{}^a$ (mult J_{HH})	$\delta_C{}^b$	$\delta_H{}^a$ (mult J_{HH})	$\delta_C{}^b$	$\delta_H{}^a$ (mult J_{HH})	$\delta_C{}^b$
1α	3.17 (dd, 6.6, 14.9)	46.4	2.81 (dd, 8.9, 14.6)	44.5	3.40 (dd, 8.2, 14.3)	47.8
1β	2.08–2.17 (m)		2.06–2.13 (m)		1.78 (m)	
2	2.24 (m)	38.2	2.44 (m)	36.0	2.36 (m)	37.6
3	5.84 (t, 3.6)	78.0	5.80 (t, 3.7)	75.9	5.77 (t, 3.4)	79.5
4	3.28 (dd, 3.6, 10.8)	49.2	2.97 (dd, 3.7, 8.1)	52.0	2.92 (dd, 3.4, 7.9)	52.9
5	6.02 (d, 10.8)	72.5	6.00 (d, 7.5)	72.4	6.37 (d, 7.9)	64.3
6		138.9		148.0		142.2
7	5.48 (dd, 3.9, 10.1)	70.8	5.11 (dd, 3.2, 9.2)	74.1	5.53 (dd, 3.1, 8.9)	78.5
8α	2.16–2.20 (m)	28.7	1.61 (m)	36.5	2.33 (m)	28.7
8β	1.61 (m)		2.38 (m)		2.21 (m)	
9	0.91 (m)	24.4	1.58 (m)	34.1	1.34 (m)	31.6
10		21.5		30.1		24.6
11	0.98 (m)	30.4	1.28 (m)	35.1	1.50 (dd, 11.0, 8.3)	27.8
12	5.77 (d, 5.6)	130.4	6.02 (d, 11.2)	136.1	6.51 (d, 11.2)	142.5
13		136.5		131.9		135.6
14		201.9		202.1		197.5
15		91.0		91.4		92.0
16	0.99 (d, 6.5)	13.7	1.07 (d, 6.7)	14.2	0.94 (d, 6.7)	14.1
17a	5.76 (s)	121.1	5.41 (s)	111.8	5.50 (s)	119.4
17b	5.61 (s)		5.00 (s)		5.22 (s)	
18	1.09 (s)	21.5	1.26 (s)	22.8	1.26 (s)	28.8
19	1.00 (s)	21.7	1.17 (s)	21.2	1.19 (s)	16.6
20	2.05 (s)	23.8	2.11 (s)	15.7	1.81 (s)	12.7
1′		165.9		166.0		166.0
2′		130.4		130.4		130.4
3′, 7′	7.96 (2H, d, 7.4)	130.0	8.16 (2H, d, 7.2)	129.7	8.06 (2H, d, 7.2)	129.7
4′, 6′	7.43 (2H, t, 7.7)	128.6	7.45 (2H, t, 7.8)	128.3	7.45 (2H, t, 7.8)	128.3
5′	7.56 (1H, t, 7.4)	133.4	7.58 (1H, t, 7.5)	133.1	7.58 (1H, t, 7.5)	133.1
1″		169.1		169.5		169.3
2″	1.48 (3H, s)	20.6	1.45 (3H, s)	20.5	1.29 (3H, s)	20.9
1‴		165.9		165.6		165.6
2‴		130.4		130.2		130.2
3‴, 7‴	7.93 (2H, d, 7.5)	129.7	8.07 (2H, d, 7.2)	129.6	7.93 (2H, d, 7.2)	129.6
4‴, 6‴	7.38 (2H, t, 7.8)	128.6	7.44 (2H, t, 7.8)	128.3	7.35 (2H, t, 7.8)	128.3
5‴	7.50 (1H, t, 7.4)	133.2	7.55 (1H, t, 7.5)	133.1	7.50 (1H, t, 7.5)	133.1
1⁗		169.2		170.0		169.7
2⁗	2.30 (3H, s)	21.6	2.07 (3H, s)	21.2	2.21 (3H, s)	21.8

^{a} Recorded at 500 MHz. ^{b} Recorded at 125 MHz.

(**3**), a major diterpenoid of the plant with a 7-hydroxy-lathyrol type macrocyclic scaffold. A further comparison of the ^{1}H and ^{13}C NMR data of **1** with those of **3** revealed identical functional groups but with differences regarding their chemical shifts. We observed upfield shifts for C-7 (δ_C 70.8, δ_H 5.48), C-9 (δ_C 24.4, δ_H 0.91), C-12 (δ_C 130.4, δ_H 5.77), and C-18 (δ_C 21.5, δ_H 1.09) and downfield shifts for C-19 (δ_C 21.7) and C-20 (δ_C 23.8, δ_H 2.05), indicating structural changes in the cyclopropyl enone of **1**. Consequently, two-dimensional NMR experiments (COSY, HSQC, HMBC, and ROESY) were used to determine the structure of **1**.

Correlations in the ^{1}H–^{1}H COSY spectrum of **1** confirmed the presence of two spin systems C-1 to C-5 and C-16 and C-7 to C-12, while HMBC correlations from H-1β (δ_H 2.08–2.17), H-3 (δ_H 5.84), H-4 (δ_H 3.28), and H-5 (δ_H 6.02) to C-15 (δ_C 91.0) revealed the presence of a five-membered ring in **1** (Fig. 2A). The correlations from H-5 and H-7 (δ_H 5.48) to C-6 (δ_C 138.9) and C-17 (δ_C 121.1) were characteristic for the presence of the exocyclic olefinic methylene group at C-6. Further HMBC correlations from H_3-18 (δ_H 1.09) and H_3-19 (δ_H 1.00) to C-9 (δ_C 24.4), C-10 (δ_C 21.5), and C-11 (δ_C 30.4) established a *gem*-dimethyl-substituted cyclopropane ring at C-9 and C-11. The assignments of the trisubstituted Δ^{12} double bond and the keto group at C-14 were determined by the correlations from H-20 (δ_H 2.05) to C-12 (δ_C 130.4), C-13 (δ_C 136.5), and C-14 (δ_C 201.9). The two acetyl groups at C-5 and C-15 were determined by the correlations from H-5 (δ_H 6.02) to C-1″ (δ_C 169.1) and from H_3-2‴′ (δ_H 2.30) to C-15. The HMBC correlations from H-3′/7′ (δ_H 7.96) and H-3 to C-1′ (δ_C 165.9) and from H-3‴/7‴ (δ_H 7.93) and H-7 to C-1‴ (δ_C 165.9) showed that the two benzoyl groups were attached to C-3 and C-7 respectively.

The relative configuration of **1** was deduced by analysis of its ^{13}C NMR and NOESY data (Fig. 2B). The *trans*-linked cyclopentane ring and the β-oriented *O*-acetyl-15, CH_3-16, and *O*-benzoyl-3 groups were deduced from the NOESY correlations between H-1β and H_3-16 (δ_H 0.99) and between H-1α (δ_H 3.17), H-2 (δ_H 2.24), H-3, and H-4 (Fig. 2B). The NOESY correlations between H-4 and H-7 and between H-5 and H-17a (δ_H 5.76) revealed that the *O*-acetyl group at C-5 was α-oriented while the *O*-benzoyl at C-7 was in β-orientation. Further NOESY correlations between H-7, H-8α (δ_H 2.16–2.20), and H-11 (δ_H 0.98) and between H-9 (δ_H 0.91) and H_3-19 indicated a *trans*-fused cyclopropane ring with a β-oriented H-9 and an α-oriented H-11. This assumption was also corroborated by the absence of a NOESY cross peak between H-9 and H-11. The (*E*)/(*Z*) double-bond geometry has a significant effect on the NMR chemical shifts of the olefinic carbons and also on the substituted carbons connected to the double bond.[20,21] In **1** the 12, 13-double bond has a (*Z*) geometry as it is indicated by an upfield-shifted carbon signal of C-12 (δ_C 130.4) and a downfield-shifted carbon signal of C-20 (δ_C 23.8). In contrast, the double bond in the *Euphorbia* factor L_2 (**3**) has the opposite (*E*) geometry. The NOESY correlation between H-12 (δ_H 5.77), H_3-20, and H_3-19 indicated furthermore the (*Z*) configuration of the trisubstituted double bond in **1**. A single crystal X-ray diffraction analysis with Cu-Kα radiation [flack parameter at 0.00(8)] (Fig. 2C) unambiguously assigned the absolute configuration of **1** as 2*S*, 3*S*, 4*R*, 5*R*, 7*R*, 9*R*, 11*S* and 15*R*. Thus, **1** was given the trivial name *Euphorbia* factor L_{2a}, and its systematic name is (2*S*, 3*S*, 4*R*, 5*R*, 7*R*, 9*R*, 11*S*, 15*R*)-5,15-diacetoxy-3,7-dibenzoyloxy-14-oxolathyra-6(17),12(13) *Z*-diene. The two specific structural characteristics of **1**, namely the (*Z*) geometry of the 12,13-double bond and the *trans*-fused cyclopropane ring at C-9/C-11 were here firstly described for the lathyrane skeleton.

Structural elucidation of *Euphorbia* factors L_{2b} (2)

Compound **2**, with a specific optical rotation of $[\alpha]_D$ +62.5 [*c* 0.46, methanol/CH_2Cl_2 (95 : 5, v/v)], had the same molecular composition as **1**. The analysis of its NMR spectroscopical data suggested that **2** was a derivative of **1** and **3** (Fig. 3A). In comparison with the ^{13}C NMR data of **1** (Table 1), the downfield-shifted carbon signal of C-12 (δ_C 136.1) and the upfield-shifted carbon signals of C-20 (δ_C 15.7) and C-13 (δ_C 131.9) suggested an (*E*)-geometry for the 12,13-double bond in **2**. The NOESY correlation of H-12 (δ_H 6.02) with H-9 (δ_H 1.58) supported the above assignment for the 12,13-double bond. The NOESY correlations H-1α (δ_H 2.81)/H-2 (δ_H 2.44), H-2/H-4 (δ_H 2.97), H-4/

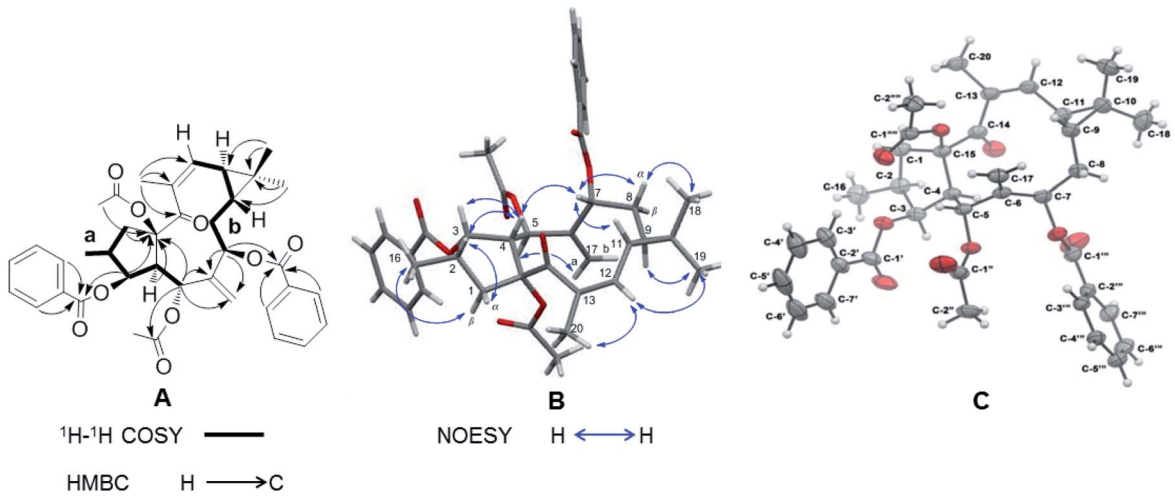

Fig. 2 (A) ^{1}H–^{1}H COSY (black thick lines) and key HMBC correlations (black arrows). (B) Important NOESY correlations (blue arrows). (C) X-ray ORTEP drawing of compound **1** (displacement ellipsoids were drawn at the 30% probability level.).

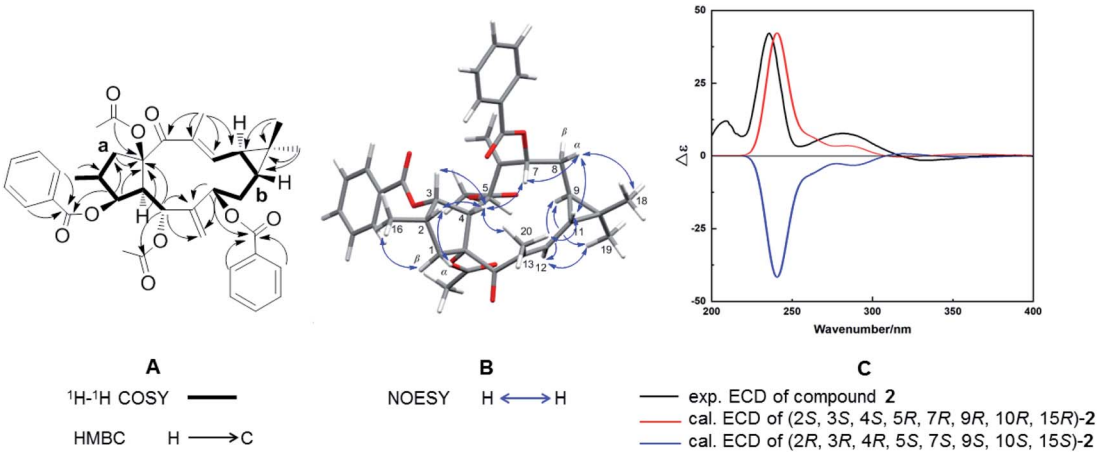

Fig. 3 (A) $^{1}H–^{1}H$ COSY (black thick lines) and key HMBC correlations (black arrows). (B) Important NOESY correlations (blue arrows). (C) Experimentally determined and calculated ECD curves of compound **2**.

H-3 (δ_H 5.80), H-4/H_3-20, H-4/H-7 (δ_H 5.11), H-7/H-8α (δ_H 1.61), H-8α/H_3-18 (δ_H 1.26), H-8α/H-11, and H-11/H_3-20 determined these hydrogens and methyl groups as cofacial and α-oriented (Fig. 3B). Further NOE correlations of H-9 (δ_H 1.58)/H-12 (δ_H 6.02), H-9/H_3-19 (δ_H 1.17), H-12/H_3-19, and H-1β (δ_H 2.11)/H_3-16 (δ_H 1.07) confirmed the β-orientation of H-9, H-12, H_3-16, and H_3-19. As a result, the cyclopropane ring was revealed to be *trans*-fused to the 11-membered ring at the positions C-9 and C-11. The relative configuration of **2** was therefore determined as (2*S**, 3*S**, 4*S**, 5*R**, 7*R**, 9*R**, 10*R**, 15*R**), resulting in a molecular structure as shown in Fig. 3B. For the absolute stereochemical determination of **2** the circular dichroism spectrum was measured and compared to the result of calculated quantum chemical electronic circular dichroism (ECD) spectra (ECD was simulated at TD-DFT/CAM-B3LYP/TZVP level). The calculated ECD curve for (2*S*, 3*S*, 4*S*, 5*R*, 7*R*, 9*R*, 10*R*, 15*R*)-**2** was in good accordance to the sign and intensity of the experimentally determined positive cotton effect (CE) at 236 and 283 nm and the negative CE at 333 nm. The calculated ECD spectrum for (2*R*, 3*R*, 4*R*, 5*S*, 7*S*, 9*S*, 10*S*, 15*S*)-**2** showed a mirror image to the experimental curve of compound **2** (Fig. 3C). Therefore, the absolute configuration of **2** was assigned to (2*S*, 3*S*, 4*S*, 5*R*, 7*R*, 9*R*, 10*R*, 15*R*). As a result, the trivial name *Euphorbia* factor L_{2b} was given to compound **2**, and its systematic description is (2*S*, 3*S*, 4*S*, 5*R*, 7*R*, 9*R*, 10*R*, 15*R*)-5, 15-diacetoxy-3,7-dibenzoyloxy-14-oxolathyra-6(17),12(13) *E*-diene.

Proposed biosynthetic pathway

Considering the structural similarities of the compounds **1–3**, these compounds may have a close biogenic relationship. We propose that *Euphorbia* factor L_2 (**3**) is the biosynthetic precursor of **1** and **2**. A plausible biosynthetic pathway for **1** and **2**, which *Euphorbia* factor L_2 triggered by light and then the formation of *trans-gem*-dimethylcyclopropane isomers (compounds **1** and **2**) through free radical intermediate, is proposed in Scheme 1.

Antitumor assay

Compounds **1–3** were tested for their *in vitro* cytotoxicity against human lung carcinoma (A549), human glioblastoma (T98G),

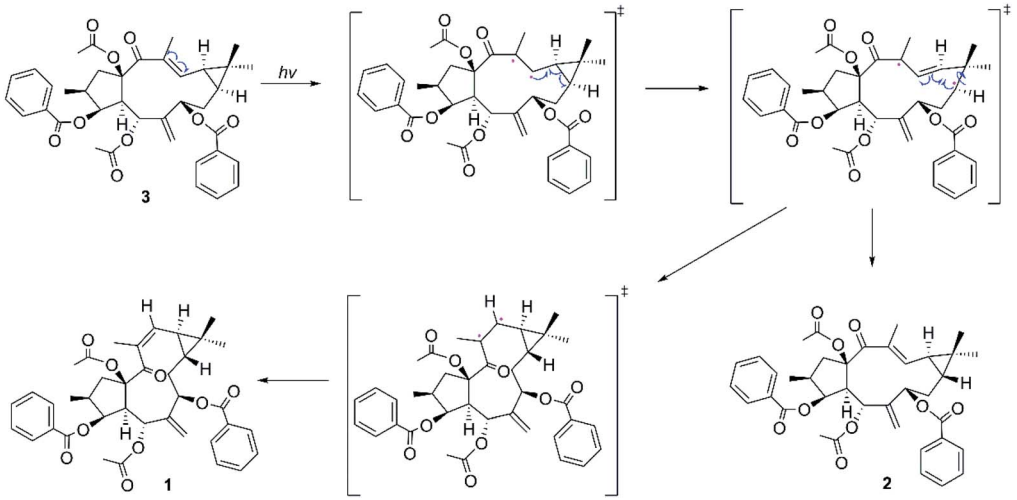

Scheme 1 Proposed biosynthetic pathway of compounds **1–2**.

Table 2 Effect of compounds **1–3** on the proliferation of T98G, A549, and U937 cells

	IC_{50} (μM)		
Compound	T98G	A549	U937
1	>200	>200	>200
2	119.71 ± 5.46	99.62 ± 3.23	0.87 ± 0.32
3	>200	>200	>200
Camptothecin	1.03 ± 0.14	0.28 ± 0.04	0.09 ± 0.02

and human leukemic monocyte lymphoma (U937) cell lines using the MTT assay. The results indicated that **1** and **3** were inactive against the above-mentioned cancer cell lines [50% effective dose of clonal inhibition (IC_{50}) > 200 μM], while **2** showed moderate cytotoxicity against U937 (IC_{50}: 0.87 ± 0.32 μM) (Table 2). It is suggested that the cytotoxicity of lathyrane-type diterpenoids is determined by the geometry of the C-12/C-13 double bond and the configuration of the cyclopropane ring in the molecule. The differential inhibitory effects against the U937 cell line of the three stereoisomers **1–3** may attract the interest of other researchers for further investigation.

Experimental

General experimental procedures

Column chromatography (CC) was performed on silica gel (200–300 mesh, Qingdao Marine Chemical Inc., China). Semi-preparative HPLC separations were conducted on a Shimadzu HPLC system (LC-20AR, Shimadzu, Japan) with a Shim-pack GIS C18 column (5 μm, 250 × 20 mm, Shimadzu, Japan). For conducting recycling preparative separations, the Shimadzu LC-20AR instrument equipped with a SPD-20A detector and an Inertsil ODS-3 column (5 μm, 150 × 10 mm, Shimadzu, Japan) was used. LC-HRMS spectra were obtained on an Agilent 6530 Q-TOF mass spectrometer coupled to an Agilent 1260 HPLC (Agilent Technologies GmbH, Waldbronn, Germany). Specific optical rotation values were measured using a Jasco P-1020 polarimeter (Jasco, Tokyo, Japan). Electronic circular dichroism spectrum was measured using a JASCO J-810 spectropolarimeter (Jasco, Tokyo, Japan) at 25 °C in spectroscopy grade methanol. NMR data were obtained using (operating at 500.13 MHz for 1H NMR and 125.75 MHz for 13C NMR) (Bruker Biospin GmbH, Karlsruhe, Germany). $CDCl_3$ was used as solvent and tetramethylsilane (TMS) was used as an internal standard. The X-ray crystallographic data were collected on a Bruker Smart Apex-II CCD diffractometer using graphite monochromated Cu-Kα radiation (λ = 1.54178 Å) at 296 *K*. SHELXT-2014 (ref. 22) was used for structure solution; SHELXL-2018 (ref. 23) for cell refinement and Mercury 4.1 (ref. 24) for the visualization of the structure.

Plant materials

The seeds of *E. lathyris* were collected from Jiaozuo in Henan Province of China in June 2016. The plants were taxonomically identified by Changqi Yuan, professor at the Institute of Botany, Jiangsu Province and Chinese Academy of Sciences. A voucher specimen (accession number 201609-EL) was deposited at the Department of Natural Product Chemistry, Institute of Botany, Jiangsu Province and Chinese Academy of Sciences.

Extraction and isolation

The dried *E. lathyris* seeds (12 kg) were extracted with 95% aqueous ethanol (50 L × 3 times × 2 hours) under reflux to give crude extracts. The combined crude extracts were evaporated under reduced pressure to yield a brown residue (5.1 kg) which was suspended in distilled H_2O (12 L) and partitioned sequentially with petroleum ether, CH_2Cl_2, and EtOAc. After evaporation of the solvent, the petroleum ether fraction (730 g) was re-extracted repeatedly with acetonitrile. The acetonitrile extract (145 g) was subjected to normal-phase silica gel CC and eluted with a petroleum ether–EtOAc gradient (1 : 0, 20 : 1, 10 : 1, 4 : 1, 2 : 1, 0 : 1, v/v) to obtain six fractions (Fr.1–Fr.6). Fraction 2 was further separated using a silica gel CC and eluted with a step-gradient (petroleum ether–EtOAc, 80 : 1, 70 : 1, 60 : 1, 50 : 1, 40 : 1, 30 : 1, 20 : 1, 10 : 1, v/v) resulting in eight subfractions (Fr.2-1–Fr.2-8). Fr.2-3 (21 g) was separated by semipreparative HPLC followed by recycling semipreparative HPLC (MeOH–H_2O, 85 : 15, v/v, 4 mL min^{-1}) to yield **1** (45 mg), **2** (20 mg) and **3** (120 mg). Recrystallization of **1** from petroleum ether–EtOAc (4 : 1) gave colorless crystals.

LC-HRMS measurements. Zorbax C18 column (3.5 μm; 150 × 4.6 mm; Agilent, St Louis, MO, USA) with a constant flow rate of 500 μL min^{-1} at 35 °C, binary solvent system of H_2O (solvent A) and MeOH (0.1% (v/v) formic acid, solvent B). 0–20 min, isocratic, 85% B; 20–30 min, isocratic, 100% B; 30–40 min, isocratic, 85% B.

***Euphorbia* factor L_{2a} (1).** Colorless crystals; $[\alpha]_D$ +20.9 [*c* 0.50, methanol/CH_2Cl_2 (95 : 5, v/v)]; HPLC-PDA-HRMS t_R 9.23 min; UV (MeOH–H_2O) λ_{max} 200, 235, 280 nm; NMR data see Table 1; HRESIMS (*m*/*z*): 665.2720 $[M + Na]^+$ (calculated for $C_{38}H_{42}O_9Na$, 665.2721). **1** was re-crystallized from petroleum ether–EtOAc (4 : 1). A single-crystal X-ray diffraction analysis using Cu-Kα radiation (λ = 1.54178 Å) was carried out to obtain the structure. $M = 642.71$, triclinic, $P\bar{1}$, $a = 9.1400(4)$ Å, $b = 9.3542(4)$ Å, $c = 10.6916(5)$ Å, $\alpha = 104.278(2)^\circ$, $\beta = 90.570(2)^\circ$, $\gamma = 91.630(2)$, $V = 885.37(7)$ Å^3, $Z = 1$, $D_c = 1.378$ mg mm^{-3}, $T = 296(2)$ K, *Flack* (abs) = 0.00(8).

***Euphorbia* factor L_{2b} (2).** Colorless crystals; $[\alpha]_D$ +62.5 [*c* 0.50, methanol/CH_2Cl_2 (95 : 5, v/v)]; HPLC-PDA-HRMS t_R 8.21 min; UV (MeOH–H_2O) λ_{max} 200, 232, 280 nm; ECD (methanol) $\lambda(\sim\Delta\varepsilon)$ 236 (+), 283 (+), 333 (−) nm; NMR data see Table 1; HRESIMS (*m*/*z*): 665.2716 $[M + Na]^+$ (calculated for $C_{38}H_{42}O_9Na$, 665.2721).

Computational details

The conformational search for a pair of enantiomers of **2** ((2*S**, 3*S**, 4*S**, 5*R**, 7*R**, 9*R**, 10*R**, 15*R**)-**2**) was performed using Spartan 14 (ref. 25) with MMFF molecular mechanics force field. After surveying the conformational space, the conformers within a 5 kcal mol^{-1} energy window were preliminarily optimized at B3LYP level using 6-31G+(d) basis set. The frequency calculation was then conducted for the previously optimized conformers to obtain the corresponding their relative Gibbs free

energies (ΔG). Boltzmann weighting factors (P_i%) for each conformer were determined on the basis of ΔG to eliminate the conformers which possess inappreciable contribution. Subsequently, the conformers selected for ECD calculation were re-optimized by DFT calculations at CAM-B3LYP/TZVP level. Then, the 20 lowest electronic transitions were calculated using time-dependent density functional theory (TD-DFT) method at CAM-B3LYP/TZVP level, and with methanol as solvent employing the PCM model. All quantum chemical calculations were conducted using Gaussian 09 program package.[26] ECD curves were generated with SpecDis[27] at a half bandwidth of 0.30 eV and 11 nm red-shift UV correction.

Biological assay

The human cancer cell lines A549, T98G, and U937 were cultured in Nutrient Mixture F-12 Ham (Sigma, USA), Dulbecco's modified Eagle's medium (Gibco, USA), and Roswell Park Memorial Institute 1640 Medium (Gibco, USA) respectively, supplemented with 10% fetal bovine serum (Gibco), 100 μg mL^{-1} penicillin, and 100 μg mL^{-1} streptomycin. All cells were cultivated in a humidified atmosphere of 5% CO_2 air at 37 °C. The cytotoxicity of compounds **1–3** against the above-mentioned three cell lines were evaluated using the 3-(4,5-dimethylthiazol-2-yl)-2,5-diphenyltetrazoliumbromide (MTT) assay, which was carried out according to protocols described previously.[28] Camptothecin was used as a positive control.

Conclusions

In conclusion, the two specific structural characteristics of the stereoisomers **1** and **2**, the (*Z*)-geometry for the C-12/C-13 double bond in **1** as well as the *trans*-fused cyclopropane ring at C-9/C-11 in **1** and **2**, are firstly found in the lathyrane skeleton. The different inhibitory effect against U937 cell lines among the three stereoisomers **1–3** may attract interest from researchers for further investigation.

Conflicts of interest

There are no conflicts to declare.

Acknowledgements

This research was supported financially by the National Natural Science Foundation of China (31770383, 31970375), the Natural Science Foundation of Jiangsu Province (BK20180311, BK20200287) and the Jiangsu Key Laboratory for the Research and Utilization of Plant Resources (JSPKLB201836). The theoretical calculations were conducted on the ScGrid and Deepcomp7000 the Supercomputing Center, Computer Network Information Center of Chinese Academy of Sciences.

Notes and references

1 A. Vasas and J. Hohmann, *Chem. Rev.*, 2014, **114**, 8579–8612.
2 M. J. Duran-Pena, J. M. Botubol Ares, I. G. Collado and R. Hernandez-Galan, *Nat. Prod. Rep.*, 2014, **31**, 940–952.
3 Y. N. Teng, Y. Wang, P. L. Hsu, G. Xin, Y. Zhang, S. L. Morris-Natschke, M. Goto and K. H. Lee, *Phytomedicine*, 2018, **41**, 62–66.
4 M. A. Reis, O. B. Ahmed, G. Spengler, J. Molnar, H. Lage and M. U. Ferreira, *J. Nat. Prod.*, 2017, **80**, 1411–1420.
5 W. Jiao, W. Dong, Z. Li, M. Deng and R. Lu, *Bioorg. Med. Chem.*, 2009, **17**, 4786–4792.
6 W. Jiao, Z. Wan, S. Chen, R. Lu, X. Chen, D. Fang, J. Wang, S. Pu, X. Huang, H. Gao and H. Shao, *J. Med. Chem.*, 2015, **58**, 3720–3738.
7 T. Yang, S. Wang, H. Li, Q. Zhao, S. Yan, M. Dong, D. Liu, X. Chen and R. Li, *Biomed. Pharmacother.*, 2020, **121**, 109663.
8 Z. G. Liu, Z. L. Li, J. Bai, D. L. Meng, N. Li, Y. H. Pei, F. Zhao and H. M. Hua, *J. Nat. Prod.*, 2014, **77**, 792–799.
9 W. Wang, Y. Wu, C. Li, Y. Yang, X. Li, H. Li and L. Chen, *Chem. Biodivers.*, 2020, **17**, e1900531.
10 A. Monico, S. Nim, N. Duarte, M. K. Rawal, R. Prasad, A. Di Pietro and M. U. Ferreira, *Bioorg. Med. Chem.*, 2017, **25**, 3278–3284.
11 A. Zhu, T. Zhang and Q. Wang, *J. Ethnopharmacol.*, 2018, **227**, 41–55.
12 J. X. Wang, Q. Wang, Y. Q. Zhen, S. M. Zhao, F. Gao and X. L. Zhou, *Chem. Pharm. Bull.*, 2018, **66**, 674–677.
13 Q. Wang, Y. Q. Zhen, F. Gao, S. Huang and X. L. Zhou, *Chem. Biodivers.*, 2018, **15**, e1800386.
14 J. W. Lee, Q. Jin, H. Jang, J. G. Kim, D. Lee, Y. Kim, J. T. Hong, M. K. Lee and B. Y. Hwang, *Chem. Biodivers.*, 2018, **15**, e1800144.
15 S. Xu, X. Zhao, F. Liu, Y. Cao, B. Wang, X. Wang, M. Yin, Q. Wang and X. Feng, *Pest Manag. Sci.*, 2018, **74**, 2716–2723.
16 H. Lyu, W. Liu, B. Bai, Y. Shan, C. Paetz, X. Feng and Y. Chen, *Molecules*, 2019, **24**, 4276.
17 S. Xu, B. Wang, L. Li, Q. Zhou, M. Tian, X. Zhao, J. Peng, F. Liu, Y. Chen, Y. Xu and X. Feng, *Pestic. Biochem. Physiol.*, 2020, **163**, 108–116.
18 Y. Chen, C. Paetz, R. C. Menezes and B. Schneider, *Phytochemistry*, 2016, **128**, 95–101.
19 G. Appendino, G. C. Tron, G. Cravotto, G. Palmisano and J. Jakupovic, *J. Nat. Prod.*, 1999, **62**, 76–79.
20 L. Hevesi, J. B. Nagy, A. Krief and E. G. Derouane, *Org. Magn. Reson.*, 1977, **10**, 14–19.
21 E. C. Chukovskaya, V. I. Dostovalova, T. T. Vasil'Eva and R. K. Freidlina, *Org. Magn. Reson.*, 1976, **8**, 229–232.
22 G. Sheldrick, *SHELXTL-2014*, University of Göttingen, Göttingen, Germany, 2014.
23 G. Sheldrick, *SHELXL-2018*, University of Göttingen, Göttingen, Germany, 2018.
24 C. F. Macrae, P. R. Edgington, P. McCabe, E. Pidcock, G. P. Shields, R. Taylor, M. Towler and J. Streek, *J. Appl. Crystallogr.*, 2006, **39**, 453–457.
25 B. Deppmeier, A. Driessen, T. Hehre, W. Hehre, J. Johnson, P. Klunzinger, J. Leonard, I. Pham, W. Pietro and J. Yu, *Spartan 14*, Wavefunction Inc., 2014.
26 M. J. Frisch, G. W. Trucks, H. B. Schlegel, G. E. Scuseria, M. A. Robb, J. R. Cheeseman, G. Scalmani, V. Barone, B. Mennucci, G. A. Petersson, H. Nakatsuji, M. Caricato, X. Li, H. P. Hratchian, A. F. Izmaylov, J. Bloino, G. Zheng, J. L. Sonnenberg, M. Hada, M. Ehara, K. Toyota, R. Fukuda, J. Hasegawa, M. Ishida, T. Nakajima, Y. Honda,

O. Kitao, H. Nakai, T. Vreven, J. A. Montgomery Jr, J. E. Peralta, F. Ogliaro, M. Bearpark, J. J. Heyd, E. Brothers, K. N. Kudin, V. N. Staroverov, R. Kobayashi, J. Normand, K. Raghavachari, A. Rendell, J. C. Burant, S. S. Iyengar, J. Tomasi, M. Cossi, N. Rega, J. M. Millam, M. Klene, J. E. Knox, J. B. Cross, V. Bakken, C. Adamo, J. Jaramillo, R. Gomperts, R. E. Stratmann, O. Yazyev, A. J. Austin, R. Cammi, C. Pomelli, J. Ochterski, R. L. Martin, K. Morokuma, V. G. Zakrzewski, G. A. Voth, P. Salvador, J. J. Dannenberg, S. Dapprich, A. D. Daniels, O. Farkas, J. B. Foresman, J. V. Ortiz, J. Cioslowski and D. J. Fox, *GAUSSIAN 09 (Revision A.1)*, Gaussian, Inc., Wallingford, CT, 2009.

27 T. Bruhn, A. Schaumlöffel, Y. Hemberger and G. Bringmann, *Chirality*, 2013, **25**, 243–249.

28 M. C. Alley, D. A. Scudiero, A. Monks, M. L. Hursey, M. J. Czerwinski, D. L. Fine, B. J. Abbott, J. G. Mayo, R. H. Shoemaker and M. R. Boyd, *Cancer Res.*, 1998, **48**, 589–601.